Investigation of the photophysical properties of a Eu^{3+} coordination polymer bearing an α-nitrile substituted β-diketonate ligand via emission and ultrafast transient absorption spectroscopy

Brodie L. Reid,[a] Evan G. Moore,[b] Brian W. Skelton,[c] Mark I. Ogden,[a,*] and Massimiliano Massi[a,*]

[a] *Department of Chemistry, and Nanochemistry Research Institute, Curtin University, Kent Street, Bentley 6102 WA, Australia.*

[b] *School of Chemistry and Molecular Biosciences, University of Queensland, St Lucia 4072 QLD, Australia.*

[c] *Centre for Microscopy, Characterisation and Analysis, University of Western Australia, Crawley 6009 WA, Australia.*

Corresponding Authors

*E-mail: m.massi@curtin.edu.au; m.ogden@curtin.edu.au.

Abstract

Reaction of the β-diketone ligand, 2-cyano-1,3-phenyl-1,3-propandione (**L**H), with hydrated $EuCl_3$ in the presence of 1,10-phenanthroline (Phen), results in the crystallisation of a one-dimensional Eu^{3+} coordination polymer of formulation, $[Eu(Phen)(\mathbf{L})_3]_\infty$, formed by coordination of the nitrile group of an O,O'-bound ligand to a neighbouring metal centre. An investigation of the metal-centred emission of the polymer, both in the solid state and solution, revealed red emission characterised by relatively long-lived excited state lifetimes and high intrinsic quantum yields. However, analysis of the overall quantum yield and sensitisation efficiency for the antenna effect reveals the ultrafast processes in the ligand potentially inhibit Eu^{3+} sensitisation. Further investigations into these processes using transient absorption spectroscopy suggest that substitution at the α-C position may significantly affect sensitisation *via* the antenna effect.

Introduction

Interest in the use of visible emitting compounds for fabrication of Organic Light Emitting Devices (OLEDs) has grown rapidly in recent years, due to the need for bright pure emissions in areas such as lighting, and plasma televisions.[1,2] The red luminescence of Eu^{3+} is of particular interest due to the sharp line-like character of its emission, giving rise to pure colours.[3–5] This emission can, however, be somewhat difficult to harness given that direct excitation of Eu^{3+} is forbidden by quantum mechanical selection rules and is therefore characterised by small absorption cross-sections.[6] This can be efficiently counteracted by use of the antenna effect, first reported by Weissman,[7] where the efficient absorption of coordinated organic molecules is exploited for the sensitisation of the lanthanoid emission. One of the most investigated ligand systems for the lanthanoids is the β-diketonate class.[8] Such research extends from the early work of Crosby and co-workers,[9,10] who studied the coordination of β-diketonate ligands to lanthanoids in solution, to the preparation of Ln^{3+} β-diketonate crystalline solids in the early 1960s.[11,12] These findings led to structural investigations of β-diketonate-lanthanoid complexes in the late 1990s and early 2000s.[13,14] More recently, interest in multinuclear lanthanoid cluster complexes supported by functionalised β-diketonate ligands has grown, resulting in the isolation of a variety of lanthanoid cluster complexes incorporating from two to 14 metal ions.[15] Furthermore, the photophysical properties of several such lanthanoid clusters have been investigated revealing characteristic red emission in the Eu^{3+} complexes.[16] Substitution of β-diketonates for lanthanoid coordination at the α-position has been reported as an effective way to reduce multiphonon relaxation and hence the overall photoluminescence quantum yield. Typical modifications include deuteration[17] at this site as well as some investigation into triketonate systems.[18,19] Merkens and Englert reported the first lanthanoid complexes bearing β-diketonates substituted at the α-C position with a –CN functionality, with structures varying from mononuclear complexes to coordination polymers.[20] These complexes contained inner sphere H_2O molecules which quench visible and near-infrared (NIR) emissions from the lanthanoids. Our work aims to improve upon this earlier work by using the 2-cyano-1,3-phenyl-1,3-propandione ligand (**L**H), in conjunction with a neutral 1,10-phenanthroline (Phen) ligand to prevent coordination of water molecules.

Results and Discussion

Synthesis

The ligand **L**H was prepared by reaction of 2-benzoylacetonitrile with benzoyl chloride in the presence of NaH in THF (Figure 1). It should be noted that after dissolution of **L**H in $CDCl_3$, the ^1H NMR spectrum does not reveal a signal for the α-proton, suggesting that the enol tautomer is the major species present, consistent with previous literature.[21]

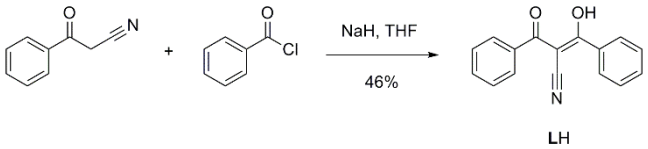

*Figure 1 – The reaction scheme for the preparation of **L**H.*

Reaction of one equivalent of both hydrated $EuCl_3$ and Phen with three equivalents of **L**H and triethylamine in ethanol, resulted in the formation of yellow crystals after slow evaporation of the solvent. The formulation of the product was determined by single crystal X-ray diffraction, revealing a coordination polymer of the formula $[Eu(Phen)(\mathbf{L})_3]_\infty$ (Figure 2). The structure observed is quite similar to a reported Ce^{3+} coordination polymer bearing 2-cyanoacetylacetonato (acacCN) ligands, however with the Phen ligand in this case replacing the two inner sphere water molecules observed for $[Ce(acacCN)_3(H_2O)_2]_\infty$.[20]

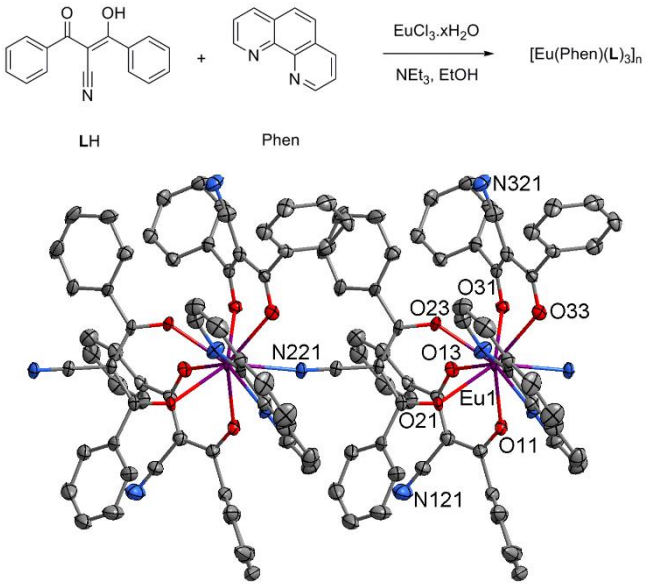

*Figure 2 – Top: Synthetic scheme of the [Eu(Phen)(**L**)$_3$]$_\infty$ complex. Bottom: Plot of the complex with displacement ellipsoids drawn at the 50% probability level. Hydrogen atoms and solvent molecules have been omitted for clarity.*

Each Eu^{3+} cation is nona-coordinated, with six O-donor atoms from three *bis*-chelating β-diketonate molecules, two N-atoms from a *bis*-chelating Phen molecule and one N-atom from a nitrile substituent of one neighbouring β-diketonate complex, thus forming a chain-like structure. The geometry of the Eu^{3+} coordination sphere was assessed using the Shape Version 2.1 software[22] and was found to be best described as a tricapped trigonal prism with dissimilar edges (see Supporting Information, Figure S1). This type of distortion has been assessed for Ln^{3+} β-diketonate complexes previously.[23]

Photophysical Properties

The energy of the lowest excited singlet state ($^1\pi\pi^*$) of the ligand **L**H was estimated by the emission spectrum of **L**H in ethanol at 77 K, and was found to lie at ~24,576 cm^{-1} (see Supporting Information, Figure S3-S4). After Gd^{3+} complexation, the emission spectrum of $\mathbf{L}^-$ was also measured at 77 K, and revealed a very similar emission trace. Hence the lowest energy triplet state ($^3\pi\pi^*$) could not be estimated in solution, suggesting that the intersystem crossing (ISC) to the triplet state is either very weak or the ligand triplet state is otherwise very short lived, due to efficient non-radiative decay pathways.

In the solid state, the [Eu(Phen)(**L**)$_3$]$_\infty$ species displays characteristic red emission. This emission originates as a consequence of the antenna effect, indicated by the broad and structureless

excitation spectrum which resembles the absorption of the $\mathbf{L}^-$ (see Supporting Information, Figure S2) and Phen[24] ligands. However the excitation spectrum also presented several sharp peaks at 465 and 535 nm, corresponding to the $^7F_0 \rightarrow {}^5D_2$ and $^7F_0 \rightarrow {}^5D_1$ intraconfigurational f-f transitions, respectively.[25] Observation of these peaks with a similar intensity compared to ligand based absorption indicates that the ligand sensitisation pathway is rather inefficient. The emission spectrum displays five line-like emission bands centred at 579, 593, 613, 650, and 694 nm, which are attributed to the Eu^{3+} metal-centred $^7F_J \leftarrow {}^5D_0$ (J = 0, 1, 2, 3, and 4) transitions, respectively. The $^7F_0 \leftarrow {}^5D_0$ transition appears as a single sharp peak of weak intensity with a full-width-half-maximum (FWHM) of ~56 cm^{-1}, indicating a single Eu^{3+} geometry in the solid state. The fine structure in the $^7F_J \leftarrow {}^5D_0$ (J = 1, 2) emission bands is consistent with a Eu^{3+} coordination geometry of a symmetry lower than C_{2v},[6,26] which agrees with that observed in the crystal structure.

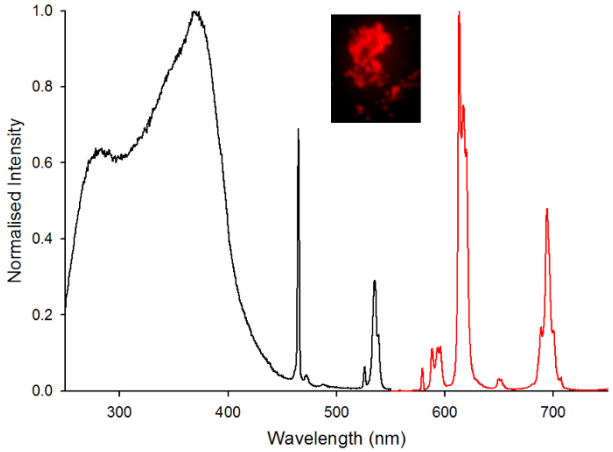

*Figure 3 – Excitation (black trace, λ_{em} = 612 nm) and emission (red trace, λ_{ex} = 350 nm) plot of [Eu(Phen)(**L**)$_3$]$_\infty$ in the solid state. Inset: Red emission observed on irradiation of the solid sample with 350 nm light.*

Excited state lifetime and photoluminescence quantum yield data are reported in Table 1. The observed luminescence lifetime (τ_{obs}) of the complex was measured in the solid state, and was best fit by a biexponential function (see Supporting Information, Figure S6) with a major component of 572 μs (90%) and a shorter minor component of 304 μs (10%). This lifetime is comparable to other β-diketonate Eu^{3+} complexes in the solid state bearing a Phen ligand.[8,27] Using the experimental τ_{obs}, it is possible to equate the radiative lifetime (τ_R), and intrinsic quantum yield (Φ^{Ln}_{Ln}), following methods proposed by Werts *et al.*[28] (see Experimental section for equations). With respect to the longer-lived τ_{obs} value, the Φ^{Ln}_{Ln} value was calculated at 35%. This value is relatively high, likely due to the Eu^{3+} coordination sphere being devoid of closely

bound high-energy quenching oscillators such as OH, thus mitigating any multiphonon relaxation pathways.

After re-dissolution of the coordination polymer in acetonitrile the emission spectrum becomes visibly different from the solid state emission at both 298 K and 77 K (Figure 4). Once again the emissions are a consequence of the antenna effect, indicated by the broad structureless excitation spectra (see Supporting Information, Figure S5). The $^{7}F_{0}\leftarrow{}^{5}D_{0}$ transition appears much broader in solution at 298 K, with a FWHM of ~100 cm^{-1} indicating flexibility in the ligand coordination in solution, which results in a more variable coordination geometry. The FWHM is reduced to ~45 cm^{-1} at 77 K, consistent with an increased rigidity of the Eu^{3+} coordination geometry in a frozen solution. On freezing the solution at 77 K, the relative intensity of the emission bands changes, however the splitting of the emission peaks do not differ significantly, which provides evidence that in a rigid matrix, the coordination geometry is different to that in the solid state, and that a nine-coordinate complex is not the major species in solution. Therefore, it is likely that in an acetonitrile solution, the coordination polymer is not preserved, and rather an eight-coordinate [Eu(Phen)(**L**)$_3$] molecular species exists. We note that a comparable change was also reported for the [Ce(acacCN)$_2$(H$_2$O)]$_\infty$ polymer, which was recrystallised from acetonitrile as the monomeric [Ce(acacCN)$_3$(H$_2$O)$_3$] complex.[20]

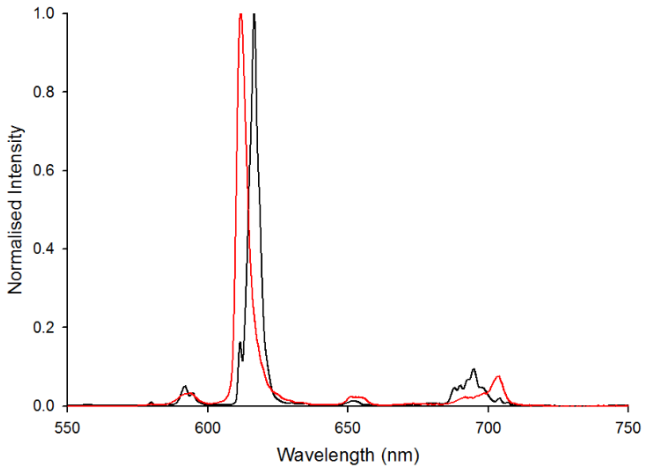

Figure 4 – Emission spectra of Eu^{3+} complex after dissolution in acetonitrile at 298K (red trace, λex = 300 nm), and 77K (black trace, λex = 350 nm).

As further evidence for this change, the τ_{obs} we observe in solution was satisfactorily fit using a monoexponential function at both 298 K and 77 K (see Supporting Information, Figure S7), and was equated to 712 and 707 µs, respectively. Elongation in the τ_{obs} value is accompanied by an increase in the Φ^{Ln}_{Ln} to 60% (298 K) and 61% (77 K). The improvement in the photophysical

properties in solution suggests that there is less quenching of the excited $^5D_0$ state, and it is possible that the formation of the monomeric species excludes the possibility of Eu···Eu cross-relaxation quenching pathways.[29] The quantum yield (Φ^L_{Ln}) of the Eu^{3+} emission in acetonitrile at 298 K was evaluated, giving a Φ^L_{Ln} of 2% after excitation at 300 nm, thus resulting in a rather low overall sensitisation efficiency (η_{sens}) of 3.4%. This outcome suggests that the sensitisation of the Eu^{3+} by the ligand $\mathbf{L}^-$ may be quite an inefficient process due to competing non-radiative deactivation pathways.

*Table 1 – Selected photophysical data for [Eu(Phen)(**L**)$_3$]$_\infty$.*

	τ_{obs} (μs)	Φ^{Ln}_{Ln} (%)[a]	Φ^L_{Ln} (%)
Solid	572 (90%) 304 (10%)	35	
MeCN 298K	712	60	2.1
MeCN 77K	707	61	

[a] See experimental section for calculation of Φ^{Ln}_{Ln}.

Transient Absorption

In an effort to rationalise the low sensitisation efficiency observed in the Eu^{3+} complex with the $\mathbf{L}^-$ ligand, we have also undertaken ultrafast transient absorption (TA) measurements on the femtosecond timescale in order to identify the photophysical processes occurring in the ligand and its lanthanoid complexes. It has been shown previously in the literature that β-diketonates display a variety of complex photoinduced processes upon electronic excitation,[30,31] and from these previous reports, we anticipated TA signals from both the S_2 ($^1\pi\pi^*$) and S_1 ($^1n\pi^*$) excited states, together with a longer lived triplet state ($^3\pi\pi^*$) often observed using TA spectroscopy.[32] Moreover, the lifetime of the latter can also be longer in the presence of Ln^{3+} ions, as a consequence of the increased rigidity in the molecule due to metal ion complexation, and in the presence of Gd^{3+} ions, the lifetime of the triplet state for structurally related compounds has been reported to be ~240 ns at room temperature.[33]

The deprotonated ligand $\mathbf{L}^-$ was investigated, as well as TA measurements after addition of excess Eu^{3+} and Gd^{3+} to a solution of $\mathbf{L}^-$ in acetonitrile. The resulting TA spectra are presented in Figure 5, with the extracted decay constants obtained from global analysis of these spectra presented in the Supporting Information (Figure S9-S11).

The TA spectrum of $\mathbf{L}^-$ reveals an initial ΔOD band with a peak at ~510 nm, which decays rapidly within the first 10 ps to form a weaker broad band spanning the visible region and with maxima at ~510 and ~575 nm. At longer time delays, the 510 nm peak continues to disappear while the red shifted component persists at time delays >50 ps, subsequently decaying more slowly to form a long lived feature which does not completely decay to zero over our observable 2.7 ns time window.

To accurately recreate the ΔOD dynamics, a four exponential decay function was required, yielding lifetime constants of τ_1 = 3.1 ps, τ_2 = 15.1 ps, τ_3 = 84.2 ps and $\tau_4 \approx$ 9.9 ns. Such multiexponential decay behaviour is not unexpected, given the highly complex photophysical processes previously observed for similar β-diketonate derivatives studied by TA in acetonitrile solution.[31] In these cases, similar multiexponential fitting procedures were required and yielded similar lifetime components [1.18 ps, 10.75 ps, 0.49 ns and >10 ns, for dibenzoylmethane (DBM)] to those we observe here for the $\mathbf{L}^-$ ligand. Hence, we have assigned the observed decay kinetics in the $\mathbf{L}^-$ ligand to fast decay of the initially formed S_2 excited state (τ_1 ~ 3.1 ps), followed by subsequent excited state decay (τ_2 ~ 15 ps) on the S_1 excited state potential energy surface, which is bifurcated, forming either a non-chelated enol *via* rotamerisation (τ_3 ~ 84 ps) or undergoing ISC to form a longer lived T_1 excited state (τ_4 ~ 8.1 ns). Notably, the assigned triplet state lifetime is much shorter compared to literature values for β-diketonates such as DBM, suggesting far more efficient non-radiative decay pathways for the excited T_1 state of the $\mathbf{L}^-$ ligand.

In the presence of Gd^{3+} ions, the TA spectra of $\mathbf{L}^-$ changes considerably, and is characterised by an initial ultrafast decay in the red from ~570-720 nm, accompanied by a negative ΔOD band centred at ~490 nm. These TA features rapidly evolve (<1ps) into a broad band at ~510 to 580 nm, which subsequently decays and red shifts at longer time delays until essentially reaching baseline over the 2.7 ns observable time window.

In this case, a three exponential decay model was able to satisfactorily reproduce the excited state decay dynamics, with resulting time constants of τ_1 = 0.4 ps, τ_2 = 3.5 ps, and τ_3 = 468.5 ps. By analogy to the free ligand, we assign the initial fast decay to $S_2 \longrightarrow S_n$ excited state absorption,

which is also accompanied in this case by strong stimulated emission (negative ΔOD) at ~490 nm. Decay of this initially populated state coincides with an increase in the TA signal at ~500-600 nm, which we attribute to $S_1 \longrightarrow S_n$ absorption, which also decays quickly with a time constant of ~2.4 ps. We assign the long lived signal to the T_1 excited state absorption, with a lifetime of $\tau_3 \approx 468.5$ ps.

Lastly, the TA spectrum of $\mathbf{L}^-$ was investigated in the presence of Eu^{3+} ions. The spectra reveal an initial broad structureless TA signal across the entire spectral window from 460-720 nm, which decays rapidly in intensity, yielding a longer lived signal which does not fully decay over the time window investigated. Applying an identical triple exponential model, we obtain decay constants of $\tau_1 = 0.4$ ps, $\tau_2 = 7.9$ ps, and $\tau_3 = 593.3$ ps which we attribute to $S_2 \longrightarrow S_n$ excited state absorption, followed by rapid internal conversion to give the $S_1 \longrightarrow S_n$ absorbing state, which undergoes ISC to form the longer lived $T_1 \longrightarrow T_n$ state with a 593.3 ps lifetime. A comparison with the Gd^{3+} complex reveals that the evaluated S_2 and S_1 excited state lifetimes are quite similar. For the excited T_1 state, however, the lifetime is in fact slightly longer lived for the Eu^{3+} complex, which is opposite to what we would have expected, given the T_1 state is typically recognised as an energy donor for sensitised Eu^{3+} emission. Given the similarity of the evaluated lifetimes for the Ln^{3+} complexes, in comparison to the $\mathbf{L}^-$ ligand, it would appear that non-radiative deactivation is a competitive deactivation pathway for the excited T_1 level, which is in agreement with the poor sensitisation properties observed for $[Eu(Phen)(\mathbf{L})_3]_\infty$ complexes in acetonitrile solution.

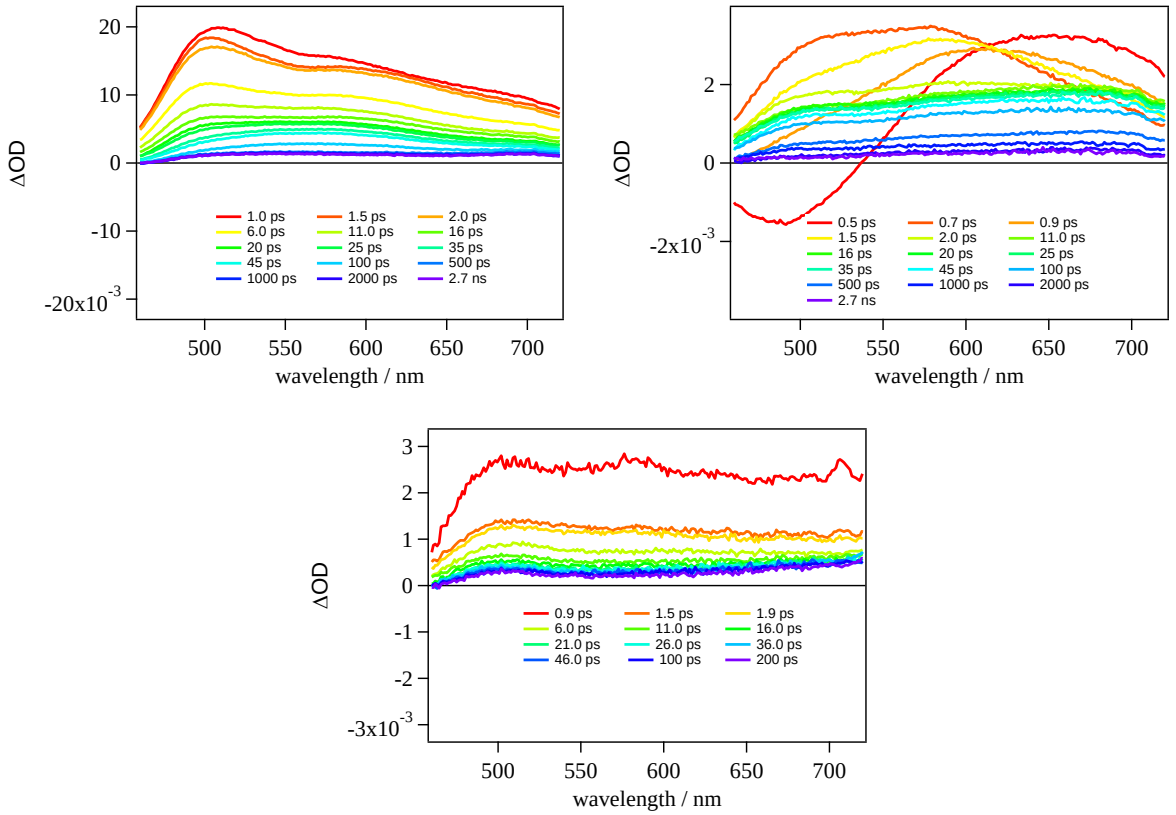

Figure 5 – Transient absorption spectra measured at various time delays (inset) after excitation (330 nm) for $\boldsymbol{L}^-$ *(top left),* $\boldsymbol{L}^-$ *with excess* Gd^{3+} *(top right), and* $\boldsymbol{L}^-$ *with excess* Eu^{3+} *(bottom).*

Conclusion

Herein, we have reported a one-dimensional Eu^{3+} coordination polymer bridged by an α-CN substituted β-diketonate ligand system, which gives characteristic red emission from the lanthanoid cation in the solid state. Re-dissolution of the complex in acetonitrile resulted in the formation of a species which has properties consistent with the mononuclear complex [Eu(Phen)(**L**)$_3$]. This solution phase complex exhibits some interesting photophysical properties. The low efficiency of sensitisation from the ligand to Eu^{3+} prompted an investigation into the ultrafast processes occurring in the ligand. Transient absorption analysis of the ligand in the presence of Ln^{3+} ions suggests that the α-CN substituted β-diketonate may not be an efficient sensitiser of Eu^{3+} emission due to efficient deactivation of its short-lived triplet state.

Experimental

General Remarks

All reagents and solvents were purchased from chemical suppliers and used as received without further purification. Benzoylacetonitrile was prepared according to a previously published procedure.[34] Hydrated $EuCl_3$ was prepared by the reaction of Eu_2O_3 with hydrochloric acid, followed by evaporation of the solvent under reduced pressure. Infrared spectra (IR) were recorded on solid state samples using an attenuated total reflectance Perkin Elmer Spectrum 100 FT-IR. IR spectra were recorded from 4000 to 650 cm^{-1}; the intensities of the IR bands are reported as strong (s), medium (m), or weak (w), with broad (br) bands also specified. Elemental analysis was obtained from elemental analysis services at the University of Tasmania.

General Photophysical Measurements

Absorption spectra were recorded at room temperature using a Perkin Elmer Lambda 35 UV/Vis spectrometer. Uncorrected steady state emission and excitation spectra were recorded using an Edinburgh FLSP980-stm spectrometer equipped with a 450 W xenon arc lamp, double excitation and emission monochromators, a Peltier cooled Hamamatsu R928P photomultiplier tube (185–850 nm). Emission and excitation spectra were corrected for source intensity (lamp and grating) and emission spectral response (detector and grating) by a calibration curve supplied with the instrument.

Excited state decays (τ) were recorded on the same Edinburgh FLSP980-stm spectrometer using a microsecond flashlamp the above-mentioned R928P PMT photomultiplier as the detector. The goodness of fit was assessed by minimizing the reduced χ^2 function and by visual inspection of the weighted residuals.

To record the luminescence spectra at 77 K, the samples were put in quartz tubes (2 mm diameter) and inserted in a special quartz Dewar filled with liquid nitrogen. The acetonitrile solvent used in the preparation of the solutions for the photophysical investigations were of spectrometric grade.

According to the approach described by Demas and Crosby,[35] the luminescence quantum yield (Φ^{L}_{Ln}) was measured in optically dilute solutions (O.D. < 0.1 at excitation wavelength) obtained from absorption spectra on a wavelength scale [nm] and compared to the reference emitter by the following equation:

$$\Phi_x = \Phi_r \frac{A_r(\lambda_r)}{A_x(\lambda_x)} \frac{I_r(\lambda_r)}{I_x(\lambda_x)} \frac{n_x^2}{n_r^2} \frac{D_x}{D_r}$$

where A is the absorbance at the excitation wavelength (λ), I is the intensity of the excitation light at the excitation wavelength (λ), n is the refractive index of the solvent, D is the integrated intensity of the luminescence and Φ is the quantum yield. The subscripts r and x refer to the reference and the sample, respectively. The quantum yield determinations were performed at identical excitation wavelength for the sample and the reference, therefore cancelling the $I(\lambda_r)/I(\lambda_x)$ term in the equation. $[Eu(Phen)(\mathbf{L})_3]_\infty$ dissolved in acetonitrile was measured against an air-equilibrated H_2O solution of $[Ru(bipy)_3]Cl_2$ used as reference ($\Phi_r = 0.028$).[36]

Transient Absorption

An amplified laser system (Spitfire ACE, Spectra Physics) was used as the excitation source, delivering *ca*. 100 fs laser pulses at 800 nm with a 1 kHz repetition rate, and transient absorption measurements were undertaken using a broad-band pump-probe transient absorption spectrometer (Helios, Ultrafast Systems). Approximately 0.1 mJ of the laser output was attenuated and focussed onto a 3 mm sapphire window to generate a white light continuum probe pulse in the visible region from 460 to 720 nm. The remainder of the laser fundamental was coupled to an OPA system (Topas Prime, Light Conversion) delivering fs tunable excitation pulses at 330 nm. The pump pulse polarisation was set to magic angle with respect to the probe, and samples with an absorbance of ~0.5-0.8 in a 2 mm pathlength (see Supporting Information, Figure S8) were continuously stirred mechanically. No detectable change was observed in the UV-Visible absorption spectrum of the sample at the completion of transient absorption studies, indicating no decomposition. The instrument response function (IRF) had a full width at half maximum (FWHM) of ca. 200 fs, measured experimentally by a Gaussian fit to the scattered laser excitation profile. All spectra were corrected for the chirp of the probe pulses, and the resulting time traces were analysed globally using commercially available software (Igor, Version 6.1.2.1, Wavemetrics). For measurements in which excess Ln^{3+} was added; lanthanoid triflates were added to a solution of **L**H with excess triethylamine in acetonitrile.

Selected Equations

Using the observed lifetimes (τ_{obs}) and calculated quantum yields (Φ^{L}_{Ln}); values of the radiative lifetime (τ_R), and intrinsic quantum yield (Φ^{Ln}_{Ln}), can be calculated following methods proposed by Werts *et al.*[28]

$$\frac{1}{\tau_R} = 14.65\ s^{-1} \times\ n^3\ \times \frac{I_{Tot}}{I_{MD}} \qquad \text{(equation 1)}$$

In equation 1, the refractive index (n) of the solvent is used (assumed value of 1.5 in the solid state),[37,38] I_{Tot} is the total integration of the Eu^{3+} emission spectrum, and I_{MD} is the integration of the $^7F_1 \leftarrow\!\!- {}^5D_0$ transition.

$$\Phi_{Ln}^{Ln} = \frac{\tau_{obs}}{\tau_R} \qquad \text{(equation 2)}$$

The sensitisation efficiency (η_{sens}) can be determined using equation 3 below:

$$\eta_{sens} = \frac{\Phi_{Ln}^{L}}{\Phi_{Ln}^{Ln}} \qquad \text{(equation 3)}$$

Synthesis

*2-Cyano-1,3-phenyl-1,3-propandione (**L**H)*

Benzoylacetonitrile (330 mg, 2.27 mmol) was added to a suspension of NaH (250 mg, 10.42 mmol) in THF (10 mL) and stirred at ambient temperature for 30 minutes. Benzoyl chloride (264 µL, 2.27 mmol) was added dropwise, and the mixture was stirred at ambient temperature overnight. Ethanol (2 drops) and water (10 mL) were added, and made acidic with HCl (1M). The mixture was extracted with ethyl acetate (10 mL), dried ($MgSO_4$), and concentrated *in vacuo*. Ethyl acetate (10 mL) and HCl (1M, 10 mL) were added to the solid, and concentrated in vacuo until a solid had precipitated in the water layer. The yellow/orange solid was collected at the pump (260 mg, 46%). ^{1}H NMR (400 MHz, $CDCl_3$): δ 7.55 (2H, m, CH), 7.66 (1H, m, CH), 8.06-8.08 (2H, d, CH). ATR-IR: *v* 3060 w, 2924 w, 2659 m, 2556 s, 2215 s, 1785 w, 1746 m, 1684 s, 1619 m, 1599 s, 1497 s, 1412 s, 1316 m, 1291 m, 1234 m, 1178 m, 1072 w, 1045 w, 1027 w, 999 w, 969 w, 928 w, 801 w, 776 w, 757 w, 733 w, 692 m, 682 m cm^{-1}.

*[Eu(Phen)(**L**)$_3$]$_\infty$*

To a mixture of hydrated $EuCl_3$ (20 mg), 1,10-phenanthroline (10 mg, 0.05 mmol), and **L**H (41 mg, 0.17 mmol) in ethanol (10 mL), triethylamine (23 µL, 0.17 mmol) was added. The resulting mixture was heated at reflux for 30 minutes. The solution was hot filtered, and left to crystallise by slow evaporation of the solvent. After *ca*. eight days, pale yellow crystals were deposited (40 mg, 86%).

M.p. 195-196°C. Anal. Calcd for $C_{60}H_{37}N_5O_6Eu\cdot(H_2O)$: C, 65.88; H, 3.59; N, 6.40. Found: C, 65.59; H, 3.68; N, 6.27. ATR-IR: *v* 3661 w, 3061 w, 2988 m, 2905 w, 2197 s, 1591 s, 1558 s, 1519 m, 1471 w, 1443 w, 1361 s, 1179 w, 1075 w, 999 w, 927 w, 863 w, 842 w, 808 w, 777 w, 698 w cm^{-1}.

X-ray Crystallography

Crystallographic data for the structures were collected at 150(2) K on an Oxford Diffraction Gemini diffractometer fitted with Mo Kα radiation**.** Following analytical absorption corrections and solution by direct methods, the structures were refined against F^2 with full-matrix least-squares using the program SHELXL-97.[39] Anisotropic displacement parameters were employed for the non-hydrogen atoms. Water molecule hydrogen atoms were not located. All remaining hydrogen atoms were added at calculated positions and refined by use of a riding model with isotropic displacement parameters based on those of the parent atom. Selected collection and refinement data are listed in the Supporting Information. CCDC-1063131 contains supplementary crystallographic data, and can be obtained free of charge *via* http://www.ccdc.cam.ac.uk/conts/retrieving.html, or from the Cambridge Crystallographic Data Centre, 12 Union Road, Cambridge CB2 1EZ, U.K.; fax: (+44) 1223-336-033; or e-mail: deposit@ccdc.cam.ac.uk

$[Eu(Phen)(\mathbf{L})_3]_\infty\cdot 0.5(H_2O)$. Empirical formula $C_{60}H_{39}EuN_5O_{6.50}$; *MW* = 1085.92. Triclinic, Space group $P\bar{1}$, *a* = 8.9578(3), *b* = 10.2101(4), *c* = 28.0127(10) Å, α = 91.280(3)°, β = 97.177(3)°, γ = 98.179(3)°, Volume = 2514.01(16) $Å^3$, *Z* = 2; ρ_c = 1.435 Mg/m^3, μ = 1.307 mm^{-1}, crystal size 0.34 x 0.16 x 0.07 mm^3; $\theta_{min,\ max}$ = 2.02, 27.50°. Reflections collected = 25976, unique reflections = 11531 [*R*(int) = 0.0521]. Max. and min. transmission = 0.910 and 0.691. Number of parameters = 658, S = 1.238; Final R indices [$I>2\sigma(I)$] *R*1 = 0.1034, *wR*2 = 0.2707; R indices (all data) *R*1 = 0.1090, *wR*2 = 0.2738; Largest diff. peak and hole 4.122 and -6.129 e. $Å^{-3}$.

Acknowledgements

M.M. (FT130100033, LE1301000052) and E.G.M. (FT100100795) wish to acknowledge financial support by the ARC. Ultrafast measurements were undertaken at the Photochemistry and Ultrafast Laser Spectroscopy (PULS≡) facility, School of Chemistry and Molecular Biosciences, established with financial support by the University of Queensland (MEI-2013000106). B.L.R. wishes to thank Curtin University for the award of an Australian Postgraduate Award scholarship. The authors acknowledge access to facilities at the Centre for

Microscopy, Characterisation and Analysis, University of Western Australia. Simon W. Lewis and Reece D. Crocker of Curtin University are acknowledged for photos of the solid state emission.

Supporting Information

The Supporting Information contains details of SHAPE Version 2.1 analysis, solution state excitation spectra, lifetime decay spectra, UV-visible absorption data, and excited state decay dynamics.

References

1 J.-C. G. Bünzli, *Acc. Chem. Res.*, 2006, **39**, 53–61.

2 J.-C. G. Bünzli and C. Piguet, *Chem. Soc. Rev.*, 2005, **34**, 1048–1077.

3 K. Binnemans, *J. Mater. Chem.*, 2009, **19**, 448–453.

4 J. P. Martins, P. Martín-Ramos, C. Coya, A. L. Alvarez, L. C. Pereira, R. Diaz, J. Martín-Gil and M. Ramos Silva, *Mater. Chem. Phys.*, 2014, **147**, 1157–1164.

5 J. P. Martins, P. Martín-Ramos, C. Coya, M. R. Silva, M. E. S. Eusebio, A. de Andrés, Á. L. Álvarez and J. Martín-Gil, *J. Lumin.*, 2015, **159**, 17–25.

6 A. de Bettencourt-Dias, *Luminescence of Lanthanide Ions in Coordination Compounds and Nanomaterials*, John Wiley & Sons Ltd, Chichester, United Kingdom, 2014.

7 S. I. Weissman, *J. Chem. Phys.*, 1942, **10**, 214–217.

8 K. Binnemans, in *Handbook on the Physics and Chemistry of Rare Earths*, 2005, vol. 35, pp. 107–272.

9 G. A. Crosby and R. E. Whan, *J. Chem. Phys.*, 1960, **32**, 614–615.

10 G. A. Crosby, R. E. Whan and R. M. Alire, *J. Chem. Phys.*, 1961, **34**, 743–748.

11 L. R. Melby, N. J. Rose, E. Abramson and J. C. Caris, *J. Am. Chem. Soc.*, 1964, **86**, 5117–5125.

12 H. Bauer, J. Blanc and D. Ross, *J. Am. Chem. Soc.*, 1964, **86**, 5125–5131.

13 L. G. Hubert-Pfalzgraf, N. Miele-Pajot, R. Papiernik and J. Vaissermann, *J. Chem. Soc., Dalton Trans.*, 1999, **9**, 4127–4130.

14 P. W. Roesky, G. Canseco-Melchor and A. Zulys, *Chem. Commun.*, 2004, 738–739.

15 P. C. Andrews, W. J. Gee, P. C. Junk and M. Massi, *New J. Chem.*, 2013, **37**, 35–48.

16 P. C. Andrews, D. H. Brown, B. H. Fraser, N. T. Gorham, P. C. Junk, M. Massi, T. G. St Pierre, B. W. Skelton and R. C. Woodward, *Dalton Trans.*, 2010, **39**, 11227–11234.

17 R. H. C. Tan, M. Motevalli, I. Abrahams, P. B. Wyatt and W. P. Gillin, *J. Phys. Chem. B*, 2006, **110**, 24476–24479.

18 M. Ismail, S. J. Lyle and J. E. Newbery, *J. Inorg. Nucl. Chem.*, 1969, **31**, 2091–2093.

19 B. L. Reid, S. Stagni, J. M. Malicka, M. Cocchi, G. S. Hanan, M. I. Ogden and M. Massi, *Chem. Commun.*, 2014, 3–5.

20 C. Merkens and U. Englert, *Dalton Trans.*, 2012, 41, 4664–4673.

21 G. I. Roshchupkina, Y. V. Gatilov, T. V. Rybalova and V. A. Reznikov, *Eur. J. Org. Chem.*, 2004, 1765–1773.

22 M. Llunell, D. Casanova, J. Cirera, P. Alemany and S. Alvarez, *Shape Version 2.1*, 2013. Available from: http://www.ee.ub.es/index.php/news-ee/575-shape-available.

23 A. Ruiz-Martínez, D. Casanova and S. Alvarez, *Chem. Eur. J.*, 2008, **14**, 1291–1303.

24 N. Armaroli, L. De Cola, V. Balzani, J.-P. Sauvage, C. O. Dietrich-Buchecker and J.-M. Kern, *J. Chem. Soc. Faraday Trans.*, 1992, 88, 553–556.

25 J.-C. G. Bünzli and S. V Eliseeva, in *Comprehensive Inorganic Chemistry II*, Elsevier, 2013, pp. 339–398.

26 S. Cotton, *Lanthanide and Actinide Chemistry*, John Wiley & Sons, Ltd, Chichester, UK, 2006.

27 J.-G. Bünzli, E. Moret, V. Foiret, K. J. Schenk, W. Mingzhao and Jin Linpei, *J. Alloys Compd.*, 1994, **207-208**, 107–111.

28 M. H. V. Werts, R. T. F. Jukes and J. W. Verhoeven, *Phys. Chem. Chem. Phys.*, 2002, **4**, 1542–1548.

29 A. Zaïm, S. V. Eliseeva, L. Guénée, H. Nozary, S. Petoud and C. Piguet, *Chem. Eur. J.*, 2014, **20**, 12172–12182.

30 L. Poisson, P. Roubin, S. Coussan, B. Soep and J. M. Mestdagh, *J. Am. Chem. Soc.*, 2008, **130**, 2974–2983.

31 P. K. Verma, A. Steinbacher, F. Koch, P. Nuernberger and T. Brixner, *Phys. Chem. Chem. Phys.*, 2015, **17**, 8459–8466.

32 C. Paris, V. Lhiaubet-Vallet, O. Jiménez, C. Trullas and M. Á. Miranda, *Photochem. Photobiol.*, 2009, **85**, 178–184.

33 S. Tobita, M. Arakawa and I. Tanaka, *J. Phys. Chem.*, 1984, **88**, 2697–2702.

34 L. Ma, L. Yuan, C. Xu, G. Li, M. Tao and W. Zhang, *Synthesis*, 2013, **45**, 45–52.

35 G. A. Crosby and J. N. Demas, *J. Phys. Chem.*, 1971, **75**, 991–1024.

36 K. Nakamaru, *Bull. Chem. Soc. Jpn.*, 1982, **55**, 2697–2705.

37 N. M. Shavaleev, S. V Eliseeva, R. Scopelliti and J.-C. G. Bünzli, *Inorg. Chem.*, 2014, **53**, 5171–5178.

38 N. M. Shavaleev, S. V. Eliseeva, R. Scopelliti and J. C. G. Bünzli, *Chem. Eur. J.*, 2009, **15**, 10790–10802.

39 G. M. Sheldrick, *Acta Crystallogr.*, 2008, **A64**, 112–122.